UV Resonance Raman and Absorption Studies of Angiotensin II Conformation in Lipid Environments

NAMJUN CHO and SANFORD A. ASHER*

Department of Chemistry, University of Pittsburgh, Pittsburgh, PA 15260

SYNOPSIS

We have used UV resonance Raman and absorption spectroscopy to examine the secondary structure of angiotensin II (AII) in aqueous solution and in phospholipid micelles. Absorption difference spectroscopic measurements are used to determine the association constant of AII with dodecylphosphocholine (DPC) micelles, and the UV Raman spectral data are used to examine the secondary structure alterations which occur upon AII partitioning into the DPC micelles. The 208 nm excited amide III peptide bands give information on the peptide backbone conformation. AII appears to exist in several conformers such as β-sheet, irregular, and turnlike structure in aqueous solution, while it adopts a more highly ordered β-turn structure in DPC micelles. The Tyr and Phe absorption and Raman excitation profile redshifts upon AII binding to DPC micelles indicate that the Tyr and Phe side chains of AII, which are exposed to water in aqueous solution, partition into the hydrophobic core of the lipid DPC micelles. © 1996 John Wiley & Sons, Inc.

INTRODUCTION

The linear octapeptide hormone angiotensin II (AII: Asp-Arg-Val-Tyr-Ile-His-Pro-Phe) is the physiologically active species in the angiotensin/renin system, which is the major regulatory system for controlling blood pressure and maintaining fluid and electrolyte homeostasis.[1] The AII humoral pressor response occurs through the stimulation of the sympathetic constriction of the circulatory and renal vasculature through stimulation of the cardiac rate, stimulation of hormone secretion by the anterior and posterior pituitary and adrenal glands, and through promotion of renal conservation of sodium and water.[1,2] Abnormalities in the AII humoral pressor response can result in hypertension.[3] The prevalence of essential hypertension in developed countries is the prime motivation for the continued pharmacological interest in the angiotensin/renin system.

The goal of the pharmacological work in this area is to design antihypertensive drugs.[4] A direct approach would be to design new drugs based on the conformation of AII at the receptor site. Unfortunately this conformational state is unknown, and present strategies attempt to infer this AII conformation by examining the conformation of AII in a variety of solvents and systems thought to mimic the receptor site. Numerous techniques have been utilized to study the AII conformation such as x-ray diffraction,[5] circular dichroism (CD),[6,7] infrared (IR),[8,9] Raman,[8,10] fluorescence[11] and two-dimensional (2D) nuclear magnetic resonance (NMR).[12] AII appears to be extremely flexible and shows various solution conformations.[13]

The conformation that AII adopts at the receptor binding site is determined by the receptor-site geometry and the bound AII local environment. This environment may at some point resemble a lipid environment or a lipid–water interface, since the AII receptor binding site appears to be at or near the epithelial plasma membrane surface of various tissues.[3] Lipid-induced peptide folding is important in peptide hormone–receptor interactions.[14–16] Little information exists on the conformation of AII in lipid environments. However, Surewicz and Mantsch's FT-IR study of the amide I′ band of AII in dimyristoylphosphatidylglycerol

* To whom correspondence should be addressed.

Biospectroscopy, Vol. 2, 71–82 (1996)
 CCC 1075-4261/96/020071-12

(DMPG)[9] suggested that the AII secondary structure mainly involves β-strands and turns.

In this work we have examined the UV resonance Raman spectra and the UV absorption spectra of AII in water and in dodecylphosphocholine (DPC) micelles to characterize the dependence of the AII conformation upon the lipid environment and to determine the portion of the AII peptide which inserts within the micelle hydrophobic core. We used absorption difference spectroscopy to determine the association constant of angiotensin II with the DPC micelles.

EXPERIMENTAL SECTION

AII was purchased from Sigma Chemical Co. (St. Louis, MO). DPC was purchased from Avanti Polar Lipids Inc. (Alabaster, AL) Gly-Tyr-Gly, Gly-Phe, Gly-His-Gly, and Gly-Pro-Gly-Gly were purchased from Research Plus Inc. (Bayonne, NJ) Cacodylic acid was purchased from Aldrich Chemical Co. (Milwaukee, WI). The AII solution pH (pD) values were adjusted by using dilute sodium hydroxide (sodium deuteroxide) and hydrochloric acid (deuterochloric acid). The pD values were obtained from pH electrode measurements corrected by utilizing the method of Glasoe and Long.[17] Solid DPC was directly added to these solutions. Above the critical micelle concentration of 1 m*M*, DPC forms micelles with an aggregation number of 40.[18]

Absorption spectra were measured by using a Perkin-Elmer Lambda 9 UV-VIS-NIR spectrophotometer. The instrumentation used for Raman measurements is described in detail elsewhere.[19-21] A Coherent Innova 300 intracavity frequency-doubled Ar^+-ion laser was used for the 229- and 238.3-nm excitation. The 457.9- and 476.5 nm Ar^+-ion lasing lines were frequency-doubled with a β-barium borate doubling crystal to give 229 and 238.3 nm, respectively.[21] A Quanta Ray Nd-YAG laser operated at 20 Hz (pulse width approximately 4 ns) was used for 220 nm excitation. The 220-nm excitation frequencies were generated by mixing the doubled-dye output with the YAG fundamental using KDP doubling and mixing crystals. A Lambda Physik model EMG 103 Excimer laser operated at 100 Hz with a pulse width of approximately 16 ns was utilized for the 208 nm excitation. The 308-nm XeCl fundamental was used to pump a Lambda Physik FL 3002 dye laser. The dye laser output was frequency-doubled with a β-barium borate doubling crystal to yield 208 nm excitation.

The excitation beam was defocussed to yield a diameter of approximately 0.6 mm at the sample. The Raman-scattered light was collected using a 150° back-scattering geometry, dispersed by a Spex Triplemate, Spex Industries, Inc. (Metuchen, NJ) spectrometer with a 1800 groove/mm spectrograph grating and detected by using a PAR OMA III, EG&G Princeton Applied Research (Princeton, NJ) detection system with a UV-enhanced intensified Reticon detector.

The sample solutions were pumped through a 1.0-mm-i.d. Suprasil, Vitro Dynamics Inc., (Rockaway, NJ) quartz capillary by using a syringe pump at the speed of approximately 5 mL/min in order to supply new sample to the illuminated volume for both CW and pulsed laser excitation. Sodium cacodylate buffer was utilized as an internal intensity standard. The absolute Raman cross section of the 607 cm^{-1} symmetric As-C stretching mode was previously determined by Song and Asher.[22] Cacodylic acid shows no Raman saturation under our experimental conditions. The absolute Raman cross sections were determined from the relative peak-height ratios of the analyte bands to that of the 607 cm^{-1} cacodylic-acid band. The relative ratios were corrected using the measured spectrometer throughput efficiency and the response sensitivity of individual detector pixel elements.

RESULTS

Figure 1 shows the absorption spectrum of an aqueous angiotensin II (AII) solution at pH 6.9 and the absorption difference spectrum in the presence and absence of DPC. The broad feature centered at 275 nm derives mainly from the Tyr $L_b \leftarrow A_{1g}$ π-π^* electronic transition, but also includes a small contribution from the Phe $L_b \leftarrow A_{1g}$ π-π^* transition centered at 257 nm.[23] The absorption increase below 240 nm is due to the strong Tyr and Phe electronic transitions, with contributions below 220 nm from His, Pro, and the peptide amide backbone π-π^* transitions.[24-26] The absorption difference spectrum shows peaks at 286.5 nm, 279 nm, and 232.5 nm, which mainly derive from Tyr. The small shoulder at 220 nm on the trough at ca. 210 nm may derive from Phe.

We have examined the environmental dependence of the Tyr and Phe side-chain absorption spectrum by measuring the absorption spectra of the model compounds Gly-Tyr-Gly [Fig. 2(A)] and Gly-Phe [Fig. 2(B)] in water and in lipid micelles. Figure 2(A) and 2(B) show the absorption spectra (■) of these species, as well as the absorp-

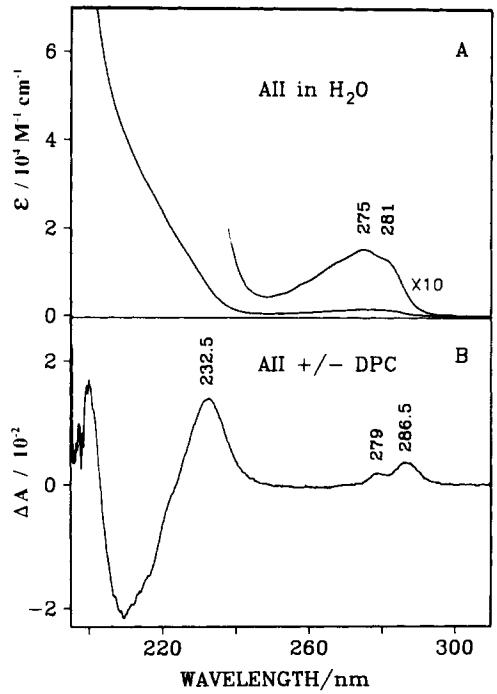

Figure 1. (A) Absorption spectrum of a 0.5-m*M* angiotensin II (AII) aqueous solution at pH 6.9 measured in a 0.5-mm cell. (B) Absorption difference spectrum induced by 39 m*M* dodecylphosphocholine (DPC).

tion difference spectra (----) in the presence and absence of DPC. Figure 2(A) also shows the absorption difference (——) and relative absorption difference spectrum (– · –) which would result from a rigid 2.5-nm absorption redshift of Gly-Tyr-Gly. The difference features produced by DPC micelle incorporation are almost identical to those calculated from a rigid 2.5-nm redshift of the Gly-Tyr-Gly absorption spectrum and closely resemble those occurring upon AII incorporation into DPC micelles (Fig. 1). From simulations of the AII absorption spectral changes, we conclude that the DPC-induced AII difference spectral peaks observed at 232.5, 279, and 286.5 nm result from a ca. 2.0-nm DPC-induced absorption redshift of the Tyr residue upon partitioning into the DPC micelle.

We have measured the absorption spectra of AII as a function of DPC concentration and have determined the association constant, $K_a = 610 M^{-1}$ (see APPENDIX). This value of K_a allows us to calculate AII values of $\Delta\epsilon_{232.5} = 1.7\ mM^{-1} \cdot cm^{-1}$ and $\Delta\epsilon_{286.5} = 0.44\ mM^{-1} \cdot cm^{-1}$; these values are close to those for Gly-Tyr-Gly [Fig. 2(A)]. For the 39-m*M* DPC concentration used in Figure 1, approximately 33% of the AII partitions into the DPC micelles, while only approximately 6% of the Gly-Tyr-Gly partitions. The AII Tyr side chain in DPC micelles has a local environment similar to that of the Gly-Tyr-Gly Tyr side chain in DPC micelles.

Figure 2(B) shows the absorption spectrum of Gly-Phe (■) in water at pH 6.9 and the difference spectrum in the presence and absence of DPC (----). Also shown is the difference spectrum (——) which would result from a rigid 1-nm absorption redshift. The L_a absorption maximum of the Gly-Phe phenyl ring occurs at 207 nm.[23] The +/− DPC difference peaks at 213 and 220 nm are similar to those which result from a 1-nm numerical redshift of the Gly-Phe absorption spectrum. The Figure 1 AII difference spectrum also shows a small shoulder near 220 nm, which probably results from a small Phe redshift upon DPC binding. Figure 2 also display the relative absorption difference spectra for Gly-Tyr-Gly and for Gly-Phe; the rela-

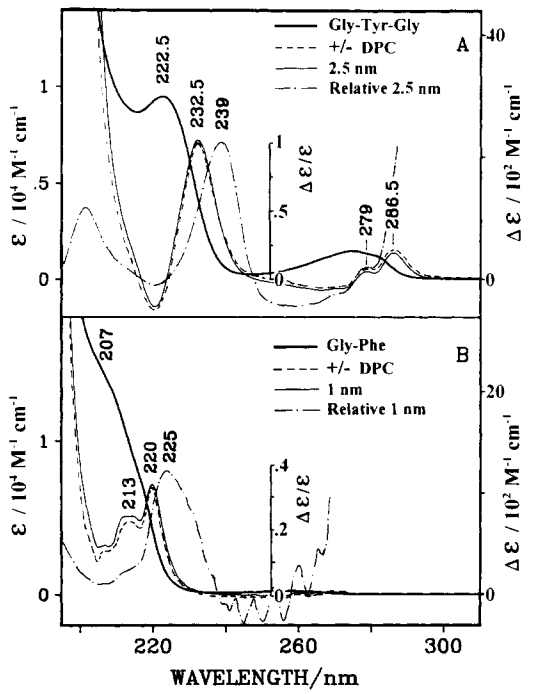

Figure 2. (A) Absorption spectrum of a 1-m*M* aqueous solution of Gly-Tyr-Gly (■) at pH 6.9 and the difference spectrum of Gly-Tyr-Gly induced by 43 m*M* DPC (----). Also shown is the difference spectrum (——) and relative difference spectrum (– · –) which would result from a rigid 2.5-nm absorption redshift. (B) Absorption spectrum of a 1-m*M* aqueous solution of Gly-Phe (■) at pH 6.9, the difference spectrum induced by 43 m*M* DPC (----) and the difference spectrum (——) and relative difference spectrum (– · –) which would result from a rigid 1-nm absorption redshift. All spectra were measured in a 0.5-mm cell.

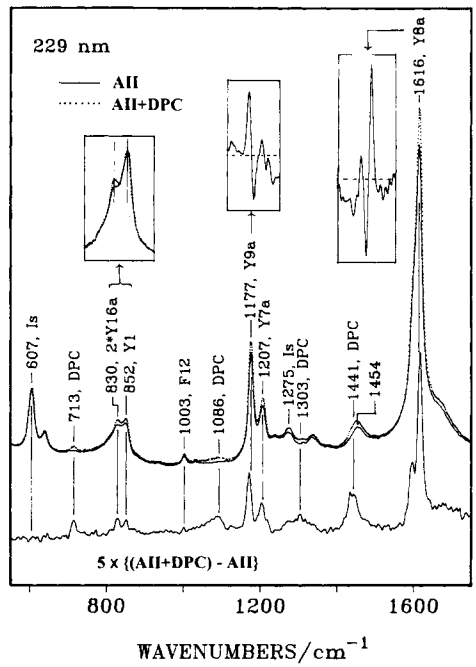

Figure 3. The 229-nm excited UV resonance Raman spectra of 1 m*M* angiotensin II in 0.1 *M* sodium cacodylate buffer at pH 6.9 in the presence (· · · · ·) and absence (——) of 43 m*M* DPC, and the Raman difference spectrum between them. The spectra were obtained by using a CW laser with a power flux of 2.5 W/cm^2 and an accumulation time of 6 min. The slit width used resulted in an 8.9-cm^{-1} spectral bandpass. The inset for 852/830 cm^{-1} bands shows an expanded view, which was obtained by subtraction of the broad 826 cm^{-1} cacodylate band and by normalization of the 852-cm^{-1} band intensity in order to clearly show the relative intensity change. The insets for 1177- and 1616-cm^{-1} bands show the calculated difference spectrum where the bands were normalized to each other in order to clearly display frequency shifts.

tive absorption difference (– · –) maxima shift to 239 and 225 nm for Tyr and Phe, respectively.

These absorption spectral changes are accompanied by Raman intensity changes. Figure 3 shows the 229-nm excited UV resonance Raman spectra of AII in 0.1 *M* sodium cacodylate buffer at pH 6.9 in the presence (· · · · ·) and absence (——) of DPC and the difference spectrum. The internal intensity standard cacodylate band at 607 cm^{-1} is used to normalize the spectra for subtraction. The Raman spectra are dominated by the strongly enhanced Tyr aromatic ring modes. The difference spectrum shows that most Tyr Raman-band intensities increase by ca. 8% upon AII binding to DPC. The most strongly enhanced Tyr Y8a band at 1616 cm^{-1} shows a 9% increased intensity with a slight frequency upshift (inset), while the Y9a 1177-cm^{-1} band and the Y7a 1207-cm^{-1} band show slight frequency downshifts (inset). The Tyr doublet band at 852 and 830 cm^{-1}, which involve a Fermi resonance between the Y1 vibration and the Y16a overtone[27] shows a decrease in the relative intensity ratio upon AII binding to DPC. The relative intensity ratio of this Fermi resonance doublet is known to be sensitive to the environment of the Tyr[28] or to the hydrogen bonding state of the Tyr phenolic hydroxyl group.[29] The 1275-cm^{-1} band mainly derives from the overlap between the cacodylate CH_3 symmetric deformation mode,[30] with a broad DPC 1303-cm^{-1} band. The Tyr Y7a′, ring C-O stretching band may also contribute. The broad band around 1454 cm^{-1} in AII derives mainly from CH_2 deformation modes of peptide side chains.[31] A DPC band at 1441 cm^{-1} overlaps this 1454 cm^{-1} AII band. Other DPC bands occur at 713, 1086, and 1303 cm^{-1}.

Figure 4 compares the 238.3-, 229-, and 220-nm UV resonance Raman spectrum of AII at pH 6.9 in the presence (· · · · ·) and absence (——) of DPC. The Tyr Raman bands dominate because these excitation wavelengths are close to the strong 222.5-nm Tyr $L_a \leftarrow A_{1g}$ absorption peak. The contribution of the Phe residue is less than 5% for 238.3- and 229-nm excitation. However, Phe Raman intensities increase for 220-nm excitation. The Phe F12 band is clearly observed at 1003 cm^{-1}, but the Phe F9a band at 1186 cm^{-1}, the F7a band at 1205 cm^{-1}, the F8b band at 1589 cm^{-1}, and the F8a band at 1607 cm^{-1} overlap with the Tyr Y9a band at 1177 cm^{-1}, the Y7a band at 1207 cm^{-1}, the Y8b band at 1601 cm^{-1}, and the Y8a band at 1616 cm^{-1}, respectively. The average contributions of Phe bands to the 220-nm excited overlapped Raman bands are expected to be ca. 30%.[23,32] The intensities of DPC bands relative to those of Tyr and Phe decrease as the excitation wavelength decreases.

The strongly enhanced Tyr 1616-cm^{-1} Y8a, 1178-cm^{-1} Y9a, and 1207-cm^{-1} Y7a bands show ca. 30% increased intensities for 238.3-nm excitation upon addition of DPC. The 229-nm excited Raman spectra shows a smaller, ca. 9%, intensity increase. In contrast the 220-nm excited Raman spectra shows an intensity decrease upon DPC addition; these data indicate that the Raman excitation profile has redshifted. This Raman excitation profile redshift is a result of the AII Tyr absorption redshift observed in Figure 1. The largest relative Raman cross-section change will occur on the red edge of the absorption band where the largest relative absorption change occurs. Similar absorption and Raman excitation profile redshifts for Tyr in

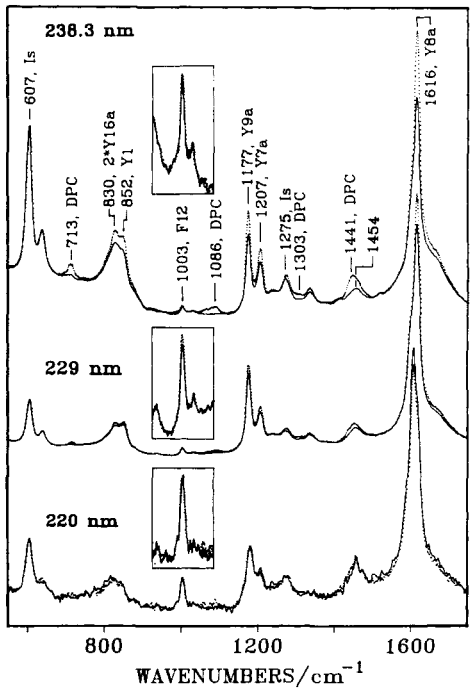

Figure 4. UV resonance Raman spectra of 1 m*M* angiotensin II in 0.1 *M* sodium cacodylate buffer at pH 6.9 in the presence (·····) and absence (——) of 43 m*M* DPC. The power flux, spectral resolution, and accumulation time were: 4.5 W/cm^2, 8.2 cm^{-1}, and 6 min. for 238.3 nm excitation; 2.5 W/cm^2, 8.9 cm^{-1}, and 6 min. for 229 nm excitation; 5.2 mJ/cm^2·pulse, 9.7 cm^{-1}, and 10 min. for 220 nm excitation. The increased intensity at 238.3 and 229 nm upon DPC addition and the decreased intensity at 220 nm show that the Raman excitation profile of Tyr redshifts upon AII binding to DPC. The insets show expanded views of the 1003-cm^{-1} Phe band in order to clearly show the intensity change. The broad overlapping DPC band at 1086 cm^{-1} is subtracted out of the 238.3- and 229-nm excited spectra.

met-hemoglobin fluoride (metHbF) were observed upon the R to T quaternary structural transition.[33] Little intensity change occurs for the Phe 1003-cm^{-1} band for 238.3-nm excitation, while intensity increases of 11% and 5% occur for 229- and 220-nm excitation, respectively. This indicates that the Phe Raman excitation profile redshifts in response to the absorption redshift observed in Figure 1. The measured Raman cross sections are listed in Table I. The cross sections for AII in DPC micelles were calculated from the Raman intensities and normalized to the relative concentration of AII which was bound to micelles. The mole fraction of AII bound to DPC micelles was 0.31, calculated from the association constant, K_a of 610 M^{-1} (see APPENDIX).

Figure 5 shows 208-nm excited UV resonance Raman spectra of AII in H_2O and in D_2O in the presence and absence of DPC. With 208-nm excitation the Phe band intensities become similar to those of Tyr. In addition, the amide bands become significantly enhanced via preresonance with the ca. 190-nm peptide backbone π-π^* transitions.[24,26] The strongest band at 1609 cm^{-1} derives from the overlap of the Phe F8a and F8b bands at 1607 cm^{-1} and 1589 cm^{-1} with the Tyr Y8a and Y8b bands at 1616 and 1601 cm^{-1}. The 1178-cm^{-1} band drives from overlap of the Tyr Y9a band at 1177 cm^{-1} with the Phe F9a band at 1186 cm^{-1}, which is more evident in D_2O solution. The 1207-cm^{-1} band mainly derives from the Tyr Y7a mode with a small contribution of Phe F7a mode at 1205 cm^{-1}.

In the amide III region, a distinct peak occurs at 1242 cm^{-1} and a very broad band appears between 1246 and 1263 cm^{-1}. This broad band may include a contribution from the Tyr Y7a′ band, which is very broad and appears around 1255–1260 cm^{-1} when the Tyr hydroxyl group is exposed to water.[34] In the amide I region, two broad shoulders occur at ca. 1660 cm^{-1}. The amide II band appears as a shoulder at ca. 1556 cm^{-1}. The weak band at ca. 1387 cm^{-1} may derive from an amide vibration containing amide C-H bending, which is enhanced due to C-C and C-N stretching contributions.[35] This band is very sensitive to the peptide backbone conformation.[26,36,37]

In D_2O solution, the strong and broad 1609-cm^{-1} band splits into two bands at 1612 and 1592 cm^{-1} due to the shifts of the Tyr Y8a and Y8b bands upon deuteration. The overlapping Phe F8a and F8b bands occur at ca. 1607 cm^{-1} and 1589 cm^{-1}, respectively. The amide I band in D_2O shifts to 1668 cm^{-1}. The amide II and III and amide C-H bending bands disappear, and are replaced by a very strong, broad band around 1420–1490 cm^{-1}, which mainly derives from the amide II′ vibration[26] with a small contribution from side-chain CH_2 deformations around 1454 cm^{-1}. The disappearance of the features between 1220 and 1290 cm^{-1} upon deuteration is proof of their assignment to the amide III vibrations. Similarly, the disappearance of the 1387-cm^{-1} band and amide II shoulder on N-D deuteration proves their assignments as well. These spectral changes are more evident in the difference spectra of Figure 6, which show the Raman difference spectrum between H_2O and D_2O for AII, and the difference spectra for AII in water in the presence and absence of DPC. The H_2O-D_2O difference spectra show the disappearance of amide III bands at 1242 and ca. 1272 cm^{-1} and the amide

Table I. Raman Cross Sections* Per Aromatic Amino Acid Residue for Angiotensin II in Aqueous Solution and Bound in DPC Micelles† for 238.3-, 229-, and 220-nm Excitations

	238.3 nm		229 nm		220 nm	
cm^{-1}	Aqueous	DPC	Aqueous	DPC	Aqueous	DPC
Phe 1003	4.84	4.84	19.8	26.9	119.5	140.5
Tyr 1177	52.2	98.7	266.0	320.8	197.8	157.2
Tyr 1207	33.0	59.4	131.3	163.9	139.2	98.6
Tyr 1616	119.0	247.4	655.2	867.8	889.4	637.5

* Units: milliBarns/molc-sr.

† The cross-sections for angiotensin II in DPC micelles were calculated from the Raman intensities and normalized to the relative concentration of angiotensin II bound to micelles.

II band at ca. 1557 cm^{-1}, and the appearance of the amide II' trough at 1468 cm^{-1}.

Addition of DPC [Figs. 5(C) and 6(A)] results in a large change in the amide III region. A small part of the spectral change could derive from the expected shift of the Tyr Y7a' 1262-cm^{-1} band to 1265 cm^{-1}, as previously observed by Takeuchi et al.,[37] when the enkephalin Tyr residue partitions into dilauryl-L-α-phosphatidylcholine membranes. The ca. 1260-cm^{-1} Y7a' band appears broad when the phenolic OH group acts as both a H-bond acceptor and donor in aqueous solution, while it sharpens and shifts to ca. 1265–1275 cm^{-1} when the phenolic OH group acts only as a H-bond donor.[34]

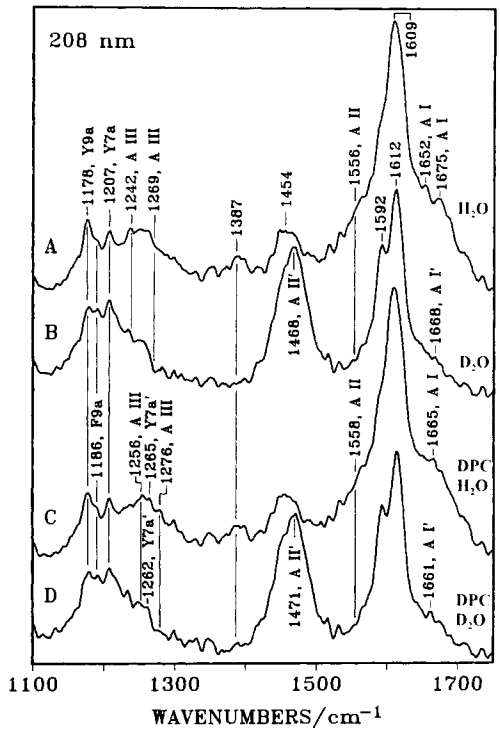

Figure 5. The 208-nm excited UV resonance Raman spectra of solutions of 0.5 m*M* angiotensin II in H_2O at pH 6.9 ([A] and [C]), and in D_2O at pD 6.9 ([B] and [D]) in the presence ([C] and [D]) and absence of 22 m*M* DPC ([A] and [B]). The energy flux, spectral resolution, and accumulation time were 3 mJ/cm^2, 10.8 cm^{-1}, and 20 min, respectively.

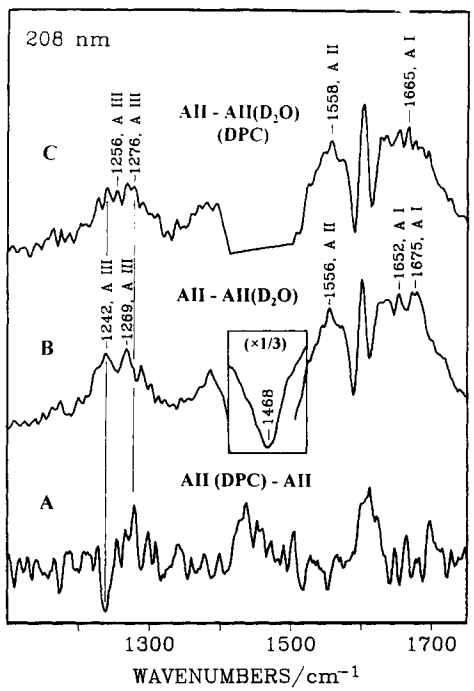

Figure 6. The 208-nm excited Raman difference spectrum of AII aqueous solution in the presence and absence of DPC (A), and the difference spectrum of AII between H_2O and D_2O in the absence (B), and presence (C) of DPC. The D_2O band at 1210 cm^{-1} is subtracted out and the strong amide II' band is truncated and shown in inset.

However, the disappearance of the 1256- and 1276-cm^{-1} bands on deuteration confirms that these bands derive from the amide III vibrations. The AII difference spectrum +/−DPC shows that the addition of DPC causes an amide III band at 1242 cm^{-1} to be replaced by an amide III band at 1276 cm^{-1}. Only small changes are evident for the broad ca. 1660-cm^{-1} amide I bands. The 1387-cm^{-1} amide band intensity appears to stay constant upon addition of DPC, but disappears in D_2O solution. The existence of the 1387-cm^{-1} amide band indicates that AII is not dominant in the α-helix conformation since this band does not occur in the α-helix form.[26]

DISCUSSION

Studies of AII analogues have determined the relative importance of individual residues in determining the biological activity. The amino acid side chains of Tyr, His, and Phe are essential for AII agonist activity.[6,38,39] Modifying the Tyr residue or replacing the Phe residue results in formation of an antagonist.[38,40] The importance of these residues could derive from their intermolecular interaction at the receptor site, or their importance could stem from their intramolecular interactions which stabilize the AII secondary structure. Obviously information on the local conformations of these side chains and their inter- and intramolecular interactions is crucial to understanding the structure–activity relationships involved upon AII binding to the receptor site.

Environment of Tyr and Phe Side Chains

The AII Raman excitation profiles and the absorption spectrum indicate that the absorption bands of Tyr and Phe side chains of AII redshift upon binding to DPC. The absorption studies of the model compounds Gly-Tyr-Gly and Gly-Phe suggest that the Tyr and Phe residues of AII in aqueous solution are exposed to H_2O; however, in the presence of DPC, the aromatic rings of Tyr and Phe in the DPC micelles reside in a more hydrophobic environment. The relatively hydrophobic Val and Ile neighboring residues probably help the Tyr residue embed in the hydrophobic region of the micelles.[41]

The recent crystallographic study of Garcia et al.[5] reports a similar conformation of AII bound to a high-affinity monoclonal antibody; the Tyr-Ile-His-Pro residues were deeply buried inside, while the carboxyl terminal residue, Phe, was located near the exterior. In the case of DPC micelles, the Phe residue appears to be embedded in the hydrophobic region of the DPC micelles, in view of the absorption and Raman excitation profile redshift of the Phe residue.

The electronic absorption change of Tyr or Phe can be caused by alterations of dipole–dipole or dipole-polarization interactions and/or hydrogen-bonding interactions.[42] An enkephalin study by Takeuchi et al.[37] similarly reported that the Tyr and Phe absorption bands redshifted and that the Raman intensities increased (240-nm excitation) due to partitioning from an aqueous to a hydrophobic environment. They explained these shifts in terms of dipole–dipole and/or dipole-polarization–interaction changes of the aromatic rings of Tyr and Phe. The ca. 1-nm absorption and Raman-excitation-profile redshift of the AII Phe residue can also be ascribed to changes in dipole–dipole and/or dipole-polarization interactions. However, the absorption redshift of the Tyr residue could also result from changes in hydrogen bonding of the phenolic hydroxyl group.[33,43]

Table II shows the dependence of the absorption spectra of N-acetyl-L-tyrosine methyl ester (Ac-Tyr-ME), p-Cresol and N-acetyl-L-phenylalanine ethyl ester (Ac-Phe-EE) upon solvent environment. The Ac-Phe-EE absorption systematically redshifts with decreasing solvent polarity.

However, the p-Cresol absorption does not simply depend on solvent polarity, but shows a very strong dependence on solvent basicity.[42] As shown in Table II, the p-Cresol absorption in cyclohexane blueshifts relative to methanol and cyclohexanol, while it slightly redshifts relative to water. This suggests that the DPC-induced AII Tyr absorption redshift could have contributions both from an increase in hydrophobicity and from an increase in the hydrogen bonding of the phenolic hydrogen. It should also be noted that the p-Cresol L_b absorption shows distinct vibronic features in cyclohexane, but not in cyclohexanol, methanol, water, or DPC micelles.

The Fermi doublet, Tyr 852- and 830-cm^{-1} relative intensity (I_{852}/I_{830}) is large when the Tyr OH group acts as a hydrogen-bond acceptor, while it decreases when the Tyr OH group acts as a hydrogen bond donor.[27–29,44] The decreased I_{852}/I_{830} intensity ratio upon AII binding to DPC (Fig. 3) signals an increase in hydrogen-bonding donation and/or a decrease in hydrogen-bonding acceptance of the Tyr phenolic OH group. Thus the observed absorption and Raman excitation profile redshifts.

Table II. Absorption Maxima of N-acetyl-L-tyrosine Methyl Ester, p-Cresol, and N-acetyl-L-phenylalanine Ethyl Ester

	π^*	$\beta^\dagger$	$\alpha^\ddagger$	Ac-Tyr-ME			p-Cresol			Ac-Phe-EE		
Water	1.09	.18	1.13	222.8	274.6	281.4	219.6	276.6	282.6	251.8	257.2	262.8
Methanol	.60	.62	.98	222.5	277.6	284.2	222.6	279.4	286	252.2	258	263.6
2-Propanol	.46	.95	.78	226.2	278.2	284.6						
Cyclohexanol							224.4	280.4	287			
Cyclohexane	0.00	0.00	0.00				220.2	278.8	285.4	252.4	258.4	264.2

* II, Scale of solvent polarity.
† β, Scale of solvent basicity.
‡ α, Scale of solvent acidity.

The decreased I_{852}/I_{830} ratio upon binding to DPC suggests that the Tyr residue of AII is buried to the hydrophobic region of the micelles and either increases its H-bonding donation or decreases its H-bonding acceptance, while the Tyr of AII aqueous solution is exposed to water and acts as a hydrogen donor and acceptor. Possibly the Tyr phenolic OH group of DPC bound AII donates a hydrogen bond to the phosphate group of DPC or the backbone carbonyl of AII. It is also possible that the Tyr residue hydrogen bonds to the imidazole ring of the His residue to form a charge-relay system.[38]

Backbone Conformation

The amide I and III Raman-band frequencies depend sensitively on the peptide or protein backbone conformation. Our ability to simultaneously use both the amide I and III bands should be extremely helpful in determining the conformational changes. This is because different interferences occur for these bands with different secondary structures; the β-sheet and β-turn amide I frequencies overlap, while in contrast the α-helix and β-turn amide III bands overlap.[44] As shown in Figures 5 and 6, however, only the amide III bands shift upon AII partitioning into the DPC micelles. This indicates that the secondary-structure alterations occur between conformations that have relatively similar amide I band frequencies and intensities. Possibly, higher S/N spectra would show changes in the amide I frequencies. It should be noted that since only 33% of the AII partitions into the micelles at the DPC concentration used, the observed change is only 33% of the real change per mole.

The relative cross-section change can be roughly estimated from the difference spectral changes observed upon deuteration. The ratio of the observed DPC-induced intensity change versus the H_2O-D_2O intensity change for amide III region is ca. 0.1. If 33% of the AII partitions into DPC micelles, ca. 30% of the amide linkages are involved in the secondary structure change which results from binding to DPC micelles. This indicates that the secondary structural changes are localized at two of the seven amide linkages, assuming that the Raman cross section of each amide III band is the same.

This Raman cross section change and the frequencies of the amide III band at 1276 cm^{-1} and amide I band at 1665 cm^{-1} strongly imply that AII adopts a β-turnlike folded structure in DPC micelles. Garcia et al.[5] also reported a very compact AII conformation containing two turns in a complex of AII and a monoclonal antibody (Mab). The main turn involves Ile, His, and Pro residues and the other turn involves Asp and Arg residues.

In aqueous solution, however, the broad amide III band around 1242 cm^{-1} and the very broad amide I band around 1675 cm^{-1} suggests the existence of a β-sheet and/or the H-bonded irregular conformation,[27,44] while the 1269-cm^{-1} amide III band and the 1652-cm^{-1} amide I band indicates a β-turn structure.[27,37,44] Also the existence of 1387-cm^{-1} amide band suggests that the major conformation of AII in aqueous solution is not α-helical.[26,35] The combined information from the amide I and III bands suggests that AII in aqueous solution adopts numerous conformations such as β-sheet, β-turn, and possibly irregular structures.

Comparison with Previous Results

The secondary structure of AII has been examined in a variety of solvents and in the lyophilized state by CD, IR Raman, fluorescence, and 2D NMR. Most of these methods agree that no α-helical structure is detected. However, numerous confor-

mations, ranging from extended coil[45,46] to β-sheet,[8] β-turn,[9,10] and γ-turn, have been reported.[38] These different conclusions may be the result of a solvent structural dependence possibly combined with a concentration dependence. An IR and Raman study conducted by Fermandjian et al.[8] suggests that AII preferentially adopts an antiparallel β-sheet conformation in both the solid state and concentrated aqueous solutions. A high-resolution protein 2D NMR study of AII in water and DMSO by Cushman et al.[12] concluded that AII adopts an extended β-sheet structure in both solvents. Our observations indicate that several different conformers exist in aqueous solution, such as irregular, β-sheet, and turnlike structure.

A FT-IR study by Surewicz and Mantsch[9] suggested that an unordered structure is a major conformer in D_2O solution, while hydrogen-bonded β-strands and turns are the main conformers in dimyristoyl phosphatidylglycerol. They concluded that an acidic phospholipid is required to cause highly ordered β-structure. However, we observed an ordered β-turnlike structure in the zwitterionic phospholipid, DPC. This suggests that acidic phospholipids, such as phosphatidylglycerol, are not critical factors for inducing conformational changes of the peptide. The two different conformations of AII in lipid environment between their study and ours may be caused by the different lipid head groups. They used only the amide I band frequencies to determine conformation. However, the amide I band frequency generally overlaps for β-turn and β-sheet structures. Recently Garcia et al.[5] reported a compact folded two-turn structure of AII complexed with a Mab. Our observations also suggest that AII adopts a folded β-turn structure in hydrophobic DPC micelles.

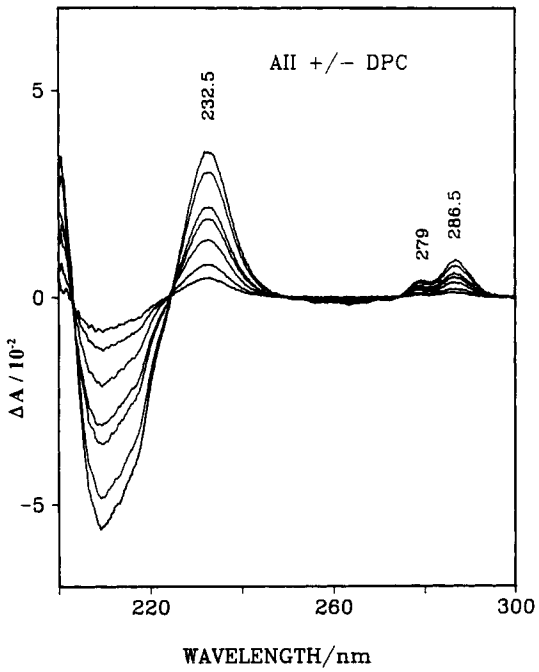

Figure 7. Absorption difference spectra of a 0.5 m*M* AII aqueous solution at pH 6.9 as a function of the added DPC. The DPC concentrations are 9.8, 20, 39, 59, 78, 170, and 280 m*M*. The absorption spectra are measured using a 0.5-mm path length quartz cell.

APPENDIX

We titrated a 0.5-m*M* solution of AII with DPC in order to determine the association constant, K_a, from the absorption difference spectra (Fig. 7). The existence of isobestic points indicates that the AII simply partitions into DPC micelles and no indication exists for more-complex situations involving AII dimers or aggregates within micelles. This permits us to develop a simple model for the AII partitioning into the DPC micelles, since we know that the DPC critical micelle concentration (CMC) is 1 m*M*, that the aggregation number is 40,[18] and that the DPC monomer concentration remains constant at concentrations above the CMC.[47,48]

The sample absorbance, A, is the sum of the absorbance of AII monomers free in water, A_f or bound in the DPC micelles, A_b. $A = A_b + A_f = l(\epsilon_b P_b + \epsilon_f P_f)$, where l is the sample pathlength and ϵ and P are the molar absorptivities and the peptide concentrations. The DPC micelle concentration is $D_N^O = (D^O - D_{CMC})/n$, where D^O is the total added DPC monomer concentration, D_{CMC} is the critical micelle concentration, and n is the aggregation number ($n = 40$). The partition equilibrium is written:

$$\text{AII} + M_{DPC} \rightleftharpoons \text{AII}\cdot M_{DPC}; \quad K_a = \frac{P_b}{P_f D_N}, \quad (1)$$

where K_a is the association constant and M_{DPC} is a DPC micelle. The initial peptide (AII) concentration is $P_O = P_b + P_f$, and the total micelle concentration is $D_N^O = D_N + P_b$, where D_N is the concentration of DPC micelle which do not contain AII. If M_F is the mole fraction of AII bound to DPC, $M_F = P_b/P_O$, the association constant can be expressed as:

$$K_a = \frac{M_F}{(1 - M_F)(D_N^O - M_F P_O)}. \quad (2)$$

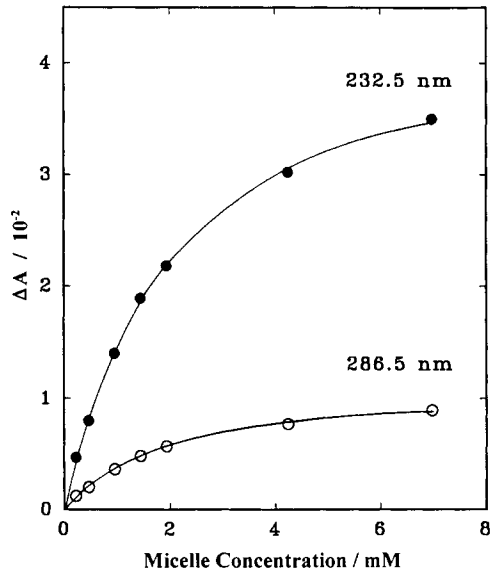

Figure 8. Plot of the absorption difference at 232.5 nm (filled circles) and at 286.5 nm (open circles) as a function of the DPC concentration. The solid curves are nonlinear least squares fit to Eq. (3).

The mole fraction of bound AII can then be written as:

$$M_F = \frac{(P_O + D_N^O + 1/K_a) - [(P_O + D_N^O + 1/K_a)^2 - 4P_O D_N^O]^{1/2}}{2P_O}, \tag{3}$$

where we neglect the unphysical positive root since $M_F = 0$ for $K_a = 0$. Given a defined AII concentration P_O, we can monitor M_F for different concentrations (i) of DPC in the difference spectrum,

$$M_{F_i} = \frac{A_i - A_O}{A_F - A_O}, \tag{4}$$

where $\Delta A_{max} = A_F - A_O$ is the saturating absorption difference at high DPC concentrations and A_O is the absorption at zero DPC concentration.

Figure 8 shows the nonlinear least squares fits to Eq. (3) for different concentrations of DPC for the absorption difference maxima which occur at 232.5 and 286.5 nm. We calculate $K_a = 610 M^{-1}$ and $\Delta\epsilon = \epsilon_b - \epsilon_f = 1.7\ mM^{-1} \cdot cm^{-1}$ at 232.5 nm, which is very close to that which results from a 2-nm red-shift of the Gly-Tyr-Gly aqueous sample solution (Fig. 2).

Our model fails if more than one AII molecule partitions into a micelle. The existence of the isobectic points indicate that if more than one AII occurs, they must not interact. This event appears unlikely. Furthermore, partitioning of more than one AII is unlikely due to the small K_a value.

We gratefully acknowledge support from NIH grant R01GM304741.

REFERENCES

1. I. Reid, B. Morris, and W. Gannong, "The renin-angiotensin system," *Ann. Rev. Physiol.*, **40,** 377 (1978).
2. J. L. Reid and P. C. Rubin, "Peptides and central neural regulation of the circulation," *Physiol. Rev.*, **67,** 725 (1987).
3. M. J. Peach, "Actions of angiotensin on elements of the vascular wall and myocardium," in *Angiotensin and Blood Pressure Regulation,* ed. by J. W. Harding, J. W. Wright, R. C. Spety, and C. D. Barnes, Academic Press, New York, 1988, p. 35.
4. P. Covol, "New therapeutic prospects of renin-angiotensin system inhibition," *Clin. Expr. Hypertens. Part A Theory Pract.*, **11,** 463 (1989).
5. K. C. Garcia, P. M. Ronco, P. J. Verroust, A. T. Brunger, and L. M. Amzel, "Three-dimensional structure of an angiotensin II-Fab complex at 3A: Hormone recognition by an anti-idiotypic antibody," *Science,* **257,** 502 (1992).
6. K. Lintner, S. Fermandjian, P. Fromageot, M. C. Khosla, R. R. Smeby, and F. M. Bumpus, "Circular dichroism studies of angiotensin II and analogues: Effects of primary sequence, solvent, and pH on the side-chain conformation," *Biochemistry,* **16,** 806 (1977).
7. F. Piriou, K. Lintner, S. Fermandjian, P. Fromageot, M. C. Khosla, R. R. Smeby, and F. M. Bumpus, "Amino acid side chain conformation in angiotensin II and analogs: Correlated results of circular dichroism and ^1H nuclear magnetic resonance," *Proc. Natl. Acad. Sci. USA,* **77,** 82 (1980).
8. S. Fermandjian, P. Fromageot, A.-M. Tistchenko, J.-P. Leicknam, and M. Lutz, "Angiotensin II conformations: Infrared and Raman studies," *Eur. J. Biochem.*, **28,** 174 (1972).
9. W. K. Surewicz and H. H. Mantsch, "Conformational properties of angiotensin II in aqueous solution and in a lipid environment: A Fourier transform infrared spectroscopic investigation," *J. Am. Chem. Soc.*, **110,** 4412 (1988).
10. J. W. Fox and A. T. Tu, "Laser Raman spectroscopic analysis of angiotensin peptides' conformation," *Arch. Biochem. Biophys.*, **201,** 375 (1980).
11. R. J. Turner, J. M. Matsoukas, and G. J. Moor, "Fluorescence properties of angiotensin II analogues in receptor-simulating environments: Relationship between tyrosinate fluorescence lifetime and biological activity," *Biochim. Biophys. Acta,* **1065,** 21 (1991).

12. J. A. Cushman, P. K. Mishra, A. A. Bothner-By, and M. S. Khosla, "Conformations in solution of angiotensin II, and its 1-7 and 1-6 fragments," *Biopolymers,* **32,** 1163 (1992).
13. R. W. Woody, in *Conformation in Biology and Drug Design* (Vol. 7 of The Peptides), ed. by V. J. Hruby, Academic Press, Orlando, 1985, p. 15.
14. B. Gysin and R. Schwyzer, "Head group and structure specific interactions of enkephalins and dynorphin with liposomes: Investigation by hydrophobic photolabeling," *Arch. Biochem. Biophys.,* **225,** 467 (1983).
15. C. M. Deber and B. A. Behnam, "Role of membrane lipids in peptide hormone function: Binding of enkephalins to micelles," *Proc. Natl. Acad. Sci. USA.,* **81,** 61 (1984).
16. D. F. Sargent and R. Schwyzer, "Membrane lipid phase as catalyst for peptide-receptor interactions," *Proc. Natl. Acad. Sci. USA,* **83,** 5774 (1986).
17. P. K. Glasoe and F. A. Long, "Use of glass electrodes to measure activities in deuterium oxide," *J. Phys. Chem.,* **64,** 188 (1960).
18. F. Inagaki, I. Shimada, K. Kawaguchi, M. Hirano, I. Terasawa, T. Ikura, and N. Go, "Structure of melittin bound to perdeuterated dodecylphosphocholine micelles as studied by two-dimensional NMR and distance geometry calculations," *Biochemistry,* **28,** 5985 (1989).
19. S. A. Asher, C. R. Johnson, and J. Murtaugh, "Development of a new UV resonance Raman spectrometer for the 217 ~ 400 nm spectral region," *Rev. Sci. Instrum.,* **54,** 1657 (1983).
20. C. M. Jones, V. L. De Vito, P. A. Harmon, and S. A. Asher, "High-repetition rate excimer-based UV laser excitation source avoids saturation in resonance Raman measurements of tyrosinate and pyrene," *Appl. Spectrosc.,* **41,** 1268 (1987).
21. S. A. Asher, R. W. Bormett, X. G. Chen, D. H. Lemmon, N. Cho, P. Peterson, M. Arrigoni, L. Spinelli, and J. Cannon, "UV resonance Raman spectroscopy using a new cw laser source: Convenience and experimental simplicity," *Appl. Spectrosc.,* **47,** 628 (1993).
22. S. Song and S. A. Asher, "Internal intensity standards for heme protein UV resonance Raman studies: Excitation profiles of cacodylic acid and sodium selenate," *Biochemistry,* **30,** 1199 (1991).
23. S. A. Asher, M. Ludwig, and C. R. Johnson, "UV resonance Raman excitation profiles of aromatic amino acids," *J. Am. Chem. Soc.,* **108,** 3186 (1986).
24. J. M. Dudik, C. R. Johnson, and S. A. Asher, "UV resonance Raman studies of acetone, acetamide, and N-methylacetamide: Models for peptide bond," *J. Phys. Chem.,* **89,** 3805 (1985).
25. R. A. Copeland and T. G. Spiro, "Secondary structure determination in proteins from deep (192–223 nm) ultraviolet Raman spectroscopy," *Biochemistry,* **26,** 2134 (1987).
26. S. Song and S. A. Asher, "UV resonance Raman studies of peptide conformation in poly(L-lysine), poly(L-glutamic acid), and model complexes: The basis for protein secondary structure determinations," *J. Am. Chem. Soc.,* **111,** 4295 (1989).
27. I. Harada and H. Takeuchi, in *Spectroscopy of Biological Systems,* ed. by R. J. H. Clark, and R. E. Hester, John Wiley & Sons, Chichester, 1986, p. 1134.
28. N. T. Yu, B. H. Jo, and D. C. O'shea, "Laser Raman scattering of cobramine B, a basic protein from cobra venom," *Arch. Biochem. Biophys.,* **156,** 71 (1973).
29. M. N. Siamwiza, R. C. Lord, M. C. Chen, T. Takamatsu, I. Harada, H. Matsuura, and T. Shimanouchi, "Interpretation of the doublet at 850 and 830 cm^{-1} in the Raman spectra of tyrosyl residues in proteins and certain model compounds," *Biochemistry,* **14,** 4870 (1975).
30. F. K. Vansant, B. J. van der Venken, and M. A. Herman, "Vibrational analysis of dimethyl arsinic acid," *Spectrochim. Acta,* **30A,** 69 (1974).
31. R. P. Rava and T. G. Spiro, "Selective enhancement of tyrosine and tryptophan resonance Raman spectra via ultraviolet laser excitation," *J. Am. Chem. Soc.,* **106,** 4062 (1984); R. P. Rava and T. G. Spiro, "Ultraviolet resonance Raman spectra of insulin and α-lactalbumin with 218 and 200 nm laser excitation," *Biochemistry,* **24,** 1861 (1985).
32. M. Ludwig and S. A. Asher, "Ultraviolet resonance Raman excitation profiles of tyrosine: Dependence of Raman cross sections on excited-state intermediates," *J. Am. Chem. Soc.,* **110,** 1005 (1988).
33. N. Cho, S. Song, and S. A. Asher, "UV resonance Raman and excited-state relaxation rate studies of hemoglobin," *Biochemistry,* **33,** 5932 (1994).
34. H. Takeuchi, N. Watanabe, Y. Satoh, and I. Harada, "Effects of hydrogen bonding on the tyrosine Raman bands in the 1300 ~ 1150 cm^{-1} region," *J. Raman Spectrosc.,* **20,** 233 (1989).
35. X. G. Chen, R. Schweitzer-Stenner, N. G. Mirkin, S. Krimm, and S. A. Asher, "N-methylacetamide and its hydrogen-bonded water molecules are vibrationally coupled," *J. Am. Chem. Soc.,* to appear.
36. Y. Wang, R. Purrello, T. Jordan, and T. G. Spiro, "UVRR spectroscopy of the peptide bond. 1. Amides, a nonhelical structure marker, is a $C_\alpha H$ bending mode," *J. Am. Chem. Soc.,* **113,** 6359 (1991).
37. H. Takeuchi, Y. Ohtsuka, and I. Harada, "Ultraviolet resonance Raman study on the binding mode of enkephalin to phospholipid membranes," *J. Am. Chem. Soc.,* **114,** 5321 (1992).
38. G. J. Moore and J. M. Matsoukas, "Conformation and chemistry of angiotensin II: Evidence for the existence of a tyrosine charge relay system in dimethylsulfoxide and water," *Eur. Pept. Symp.,* 615 (1984); G. J. Moore, and J. M. Matsoukas, "Angiotensin as a model for hormone-receptor interactions," *Biosci. Rep.,* 407 (1985).

39. P. R. Bovy, D. P. Getman, J. M. Matsoukas, and G. J. Moore, "Influence of polyfluorination of the phenylalanine ring of angiotensin II on conformation and biological activity," *Biochim. Biophys. Acta,* **1079,** 23 (1991).
40. A. Aumelas, C. Sakarellos, K. Lintner, S. Fermandjian, M. C. Khosla, R. R. Smeby, and F. M. Bumpus, "Studies on angiotensin II and analogs: Impact of substitution in position 8 on conformation and activity," *Proc. Natl. Acad. Sci. USA,* **82,** 1881 (1985).
41. D. M. Engelman, T. A. Steitz, and A. Goldman, "Identifying nonpolar transbilayer helices in amino acid sequences of membrane proteins," *Ann. Rev. Biophys. Biophys. Chem.,* **15,** 321 (1986).
42. M. J. Kamlet, G. L. M. Abboud, and R. W. Taft, "An examination of linear solvation energy relationships," *Prog. Phys. Org. Chem.,* **13,** 485 (1981).
43. K. R. Rodgers, C. Su, S. Subramaniam, and T. G. Spiro, "Hemoglobin R → T structural dynamics from simultaneous monitoring of tyrosine and tryptophan time-resolved UV resonance Raman signals," *J. Am. Chem. Soc.,* **114,** 3697 (1992).
44. A. T. Tu, in *Spectroscopy of Biological Systems,* ed. by R. J. H. Clark and R. E. Hester, John Wiley & Sons, Chichester, 1986, p. 47.
45. J. M. Matsoukas, G. Bigham, N. Zhou, and G. J. Moore, "^{1}H-NMR studies of [Sar^1]angiotensin II conformation by nuclear overhauser effect spectroscopy in the rotating frame (ROESY): Clustering of the aromatic rings in dimethylsuloxide," *Peptides,* **11,** 359 (1990).
46. N. Zhou, G. J. Moor, and H. J. Vogel, "Proton NMR studies of angiotensin II and its analogs in aqueous solution," *J. Protein Chem.,* **10,** 333 (1991).
47. N. J. Turro and A. Yekta, "Luminescent probes for detergent solutions. A simple procedure for determination of the mean aggregation number of micelles," *J. Am. Chem. Soc.,* **100,** 5951 (1978).
48. J. H. Fendler, *Membrane Mimetic Chemistry,* Wiley, Chichester, 1982.

Received July 10, 1995
Revised September 14, 1995
Accepted December 18, 1995